7

Distance evaluation between vehicle trajectories and risk indicator

Abdourahmane KOITA and Dimitri DAUCHER
LEPSIS/LCPC (Laboratoire Central des Ponts et Chaussées)
58, Boulevard Lefebvre 75015 Paris, France

1. Introduction

This study, dealing with the vehicle trajectories modeling, is a subject of a scientific research in our *Laboratory*, within the framework of a research program on road safety. For many years, road accidents have been the focus of attention of the authorities and vehicle manufacturers. The accidents due to the vehicle loss control have very serious consequences in human terms (WHO, 2004).
In the literature, the first research works on the vehicle loss control risk consisted in defining a critical failure speed in a bend or a speed profile to be respected according to the road geometrical characteristics and the vehicle dynamic state (Lauffenburger, 2003). Other works in progress consist of using a dynamic vehicle model, to carry out an analysis of sensitivity in order to determine the most influential parameters on the answer of this model.
In addition, the LCPC (Laboratoire Central des Ponts et Chaussées) launched a research operation MTT (Métrologie des Trajectoires et du Trafic) and the research projects SARI/RADARR and DIVAS. Within this framework, several observatories of vehicle's trajectories (edge of way or instrumented vehicle) in bend were developed then deployed in order to analyze the trajectory stability and to understand how it would be possible to detect a failing trajectory.

In this study, we developed a new method to evaluate risk of trajectory failure by using experimental data measurements. The method consists of defining a metric (or distance) able to compare trajectories each other in order to evaluate the handling loss risk. Then we determined the limit states (or the critical sections) which govern the intersection between Vehicle, Infrastructure and Driver (V/I/D) in the safety trajectory space. Indeed the very complex systems (with several configurations variables) and a strongly constrained environment can cause failure modeling of many algorithms, due to their complexity.
However the probabilistic trajectories modeling are used in order to estimate the risk indicator. It consists in considering some parameters as random variables in order to take into account the risks induced to the infrastructure, the vehicle, the behavior of the driver and the environment (weather or traffic). Lastly, we will calculate the probability of going beyond of the threshold applied to the distance.

The results can also be used on the one hand: to find the characteristics of the infrastructure which will be modified in order to minimize the lane crossing risk, and in addition: to warn the driver by detecting the failure trajectory. The originality of this method is not only the use of a particular norm (taking into account the vehicle position, velocity and acceleration) to compare trajectories between them, but also the use of reliability analysis of the vehicle trajectories.

In this chapter, after the introduction, in the first part, we define vehicle's trajectory as a vectorial stochastic process. In the second part, a functional filter (Mahalanobis distance and Euclidean distance) judiciously chosen are used to project on IR the set of the observed trajectories in order to get a stationary scalar process. In Third part, we will use a statistic analysis on our scalar process in order to characterize and to identify it. Then, one identifies the whole of the parameters intervening in each limit state by using the constraints applied to the vehicle. Lastly, we will use reliability analysis method to build a risk indicator. The approach consists of drawing lots configurations at random by probability laws and to connect between them to generate an ideal trajectory. We will calculate their probability function. Then with the already defined safety margin, we make the comparison of the probability obtained in that admitted preliminary. The safety margin which bounds the failure domain to the safety domain is determined by the limit state function. The risk of lane crossing is quantified by the risk indicator (reliability) estimate.

2. Vehicle trajectory definition

2.1 Deterministic function

The vehicle trajectory, during an amount of time $T = [0, \tau]$ is the resultant of an interaction between vehicle, infrastructure and driver. It can be defined by the knowledge of the following deterministic function:

$$\Phi : \mathrm{T} \rightarrow \mathrm{IR}^6$$
$$\mathrm{t} \mapsto \Phi(\mathrm{t}) = \left(\mathrm{x(t)}, \mathrm{y(t)}, \frac{\partial \mathrm{x}}{\partial \mathrm{t}}(t), \frac{\partial y}{\partial \mathrm{t}}(t), \frac{\partial^2 \mathrm{x}}{\partial \mathrm{t}^2}(t), \frac{\partial^2 y}{\partial \mathrm{t}^2}(t) \right) \quad (1)$$

Where the parameters of function Φ(t) represented the vehicle longitudinal position, the lateral position, the longitudinal velocity, the lateral velocity , the longitudinal acceleration and the lateral acceleration. The sample $\{x_k, k \in K_N\}$ is considered as a discretized trajectory of a two-dimensional second order mean-square continuous, at times $\{t_k, k \in K_N\}$.
However, the behavior of the dynamical system to investigate is fundamentally nonlinear. It expresses the dynamics of a system whose mechanical behaviour and connections are very complex. Consequently, it is necessary to take into account various levels of uncertainty (uncertainty of measurements, risks on control,…). For example, the same driver circulating with the same vehicle on the same road under the same conditions will not twice reproduce the same trajectory within the meaning of (1). Obviously, it's very important and necessary to take into account this random part.

2.2 Vectorial stochastic process

It is thus more judicious to model the trajectories of a triptych V-I-D (Vehicle, Infrastructure, Driver), by realizations of a vectorial stochastic process (Koita et al., 2008) in the following form:

$$\widetilde{U} : \mathrm{T}\times\Omega\rightarrow \mathrm{IR}^6$$
$$(\mathrm{t},\omega)\mapsto\widetilde{U}(\mathrm{t},\omega)=\left(\mathrm{x}(\mathrm{t},\omega),\mathrm{y}(\mathrm{t},\omega),\frac{\partial \mathrm{x}}{\partial \mathrm{t}}(t,\omega),\frac{\partial y}{\partial \mathrm{t}}(t,\omega),\frac{\partial^2 \mathrm{x}}{\partial \mathrm{t}^2}(t,\omega),\frac{\partial^2 y}{\partial \mathrm{t}^2}(t,\omega)\right) \quad (2)$$

where Ω is the realizations space.

As soon as the driver changes, the experimental trajectories collected are discrete realizations of different stochastic processes. From this definition, we use a database of trajectories. This database is made up of L realizations of experimental trajectories resulting from the same vectorial stochastic process noted U of the form :

$$U : \mathrm{T}\times\Omega\rightarrow \mathrm{IR}^6$$
$$(\mathrm{t},\omega)\mapsto U(\mathrm{t},\omega)=\left(\mathrm{x}(\mathrm{t},\omega),\mathrm{y}(\mathrm{t},\omega),\frac{\partial \mathrm{x}}{\partial \mathrm{t}}(t,\omega),\frac{\partial y}{\partial \mathrm{t}}(t,\omega),\frac{\partial^2 \mathrm{x}}{\partial \mathrm{t}^2}(t,\omega),\frac{\partial^2 y}{\partial \mathrm{t}^2}(t,\omega)\right) \quad (3)$$

The reader will find in (Koita, 2008) more complete information on the experimental observations and especially methodology used to say that the trajectories considered result from the same stochastic process. To illustrate our remarks on the trajectories observed, the figure (1) represent a realization of the process.

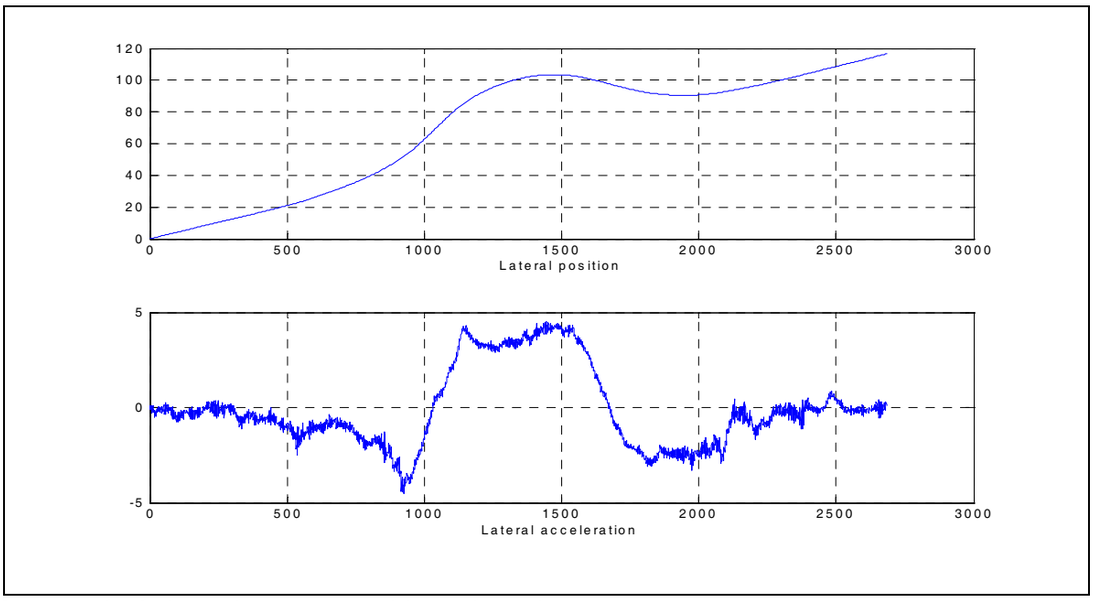

Fig. 1. Vehicle lateral position and lateral acceleration

The trajectories of the studied process represent a behavior of control identified on a given turn. The final goal of this study being to analyze the risk of failed trajectory, therefore we

choose to work on the behavior of control of fast trajectories. The drivers having realized these trajectories were considered in a normal stress state at the time of the experimentation.

From this definition of the vehicle trajectory, a particular trajectory was defined with the aim of comparing later, all the observed trajectories to this particular trajectory. This particular trajectory will be regarded as reference trajectory for all the study.

2.3 Reference Trajectory

There exists in the literature several work concerning the reference trajectory for example (Lauffenburger et al, 2000) predict the reference trajectory by the splines method according to the road reference frame and a behavioral model of the driver. The reference trajectory considered in this study is the average function of the whole of the trajectories.

$$\begin{aligned} m_U &: \mathrm{IR} \to \mathrm{Mat}_{\mathrm{IR}}(6,1) \\ (\mathrm{t}) &\mapsto m_U(\mathrm{t}) = \overline{U}(t) = \frac{1}{L}\sum_{\mathrm{l}=1}^{\mathrm{L}} \mathrm{U(t)} \end{aligned} \tag{4}$$

This choice is justified on the one hand, in the data measurements where we note that most of the drivers roll while following the road center and on the other hand, the distance which we will use later in this study to compare trajectories between them. It is a distance which estimates the difference between a variable and its median value. The average trajectory can be also justified as trajectory of reference because not only it grants more weight in the majority of the observed trajectories having similar values but also it remains sensitive to all the trajectories observed of the turn in particular to the extreme trajectories. What is useful and necessary to take account of all the information delivered by the turn and received by the drivers (perception of the road).

After having defined the vehicle trajectory like vectorial stochastic process, no one needs a statistical analysis of this process. But before that, the other studies on the same database showed the partial stationary of a parameter or several parameters at the same time but never a complete stationarity of all the parameters of the trajectory at the same time. The same studies showed that none stationarity of this process comes at the same time from the none stationarity of its moments (the average μ, the standard deviation σ, etc).

From now, we will make a projection of this vectorial process on a functional filter. The goal of this projection is not only to work on a scalar process easy to analyze but especially to obtain a stationary scalar process. The important role of the stationarity of the process is the interval of prediction of the failure of the trajectory is different compared to an evolutionary process.

3. Distance evaluation between trajectories

We noted through the first observations on the measurements data, that the trajectory parameters are not stationary throughout the turn, because as soon as the driver changes, the experimental trajectories collected are discrete realizations of a different process. To

conclude, it is obviously necessary to be placed within a framework where one lays out of observations of the same process of sufficient number. The goal of this section will be to transform our vectorial process U in scalar process making a projection without losing the information contained in the system interaction (V/I/D).

Starting from this sample (or class) of trajectories having similar statistical properties, it will be advisable to analyze statistically the scalar process D_i =g(U) where i={E,M}. This implies the use of a suitable topological distance, the choice was made on the Mahalanobis distance D_M (Xinrong, 2001) and the Euclidean distance D_E (Lanequel, 1992), with standard variables.

This approach of modeling consists of considering the distance like a realization during the time of a process. One regards the trajectory parameters as random in order to taking into account of the risks relating to the infrastructure, vehicle, driver and environment (weather or traffic).

3.1 Euclidean distance (norm)

It is a distance in the Euclidean metric space whose characteristic is to grant the same weight to all the components of the vector or the matrix. It is defined by the following equation:

$$D_E = d\left(U, \overline{U}\right) = \sqrt{\left(U - \overline{U}\right)\left(U - \overline{U}\right)^T} \tag{5}$$

This distance obtained is a scalar and its major disadvantage is to not taken into account of the correlation between components (in our case, the trajectory parameters). The projection of a vectorial process U(t) give a scalar process $D_E(t)$ defined by:

$$\begin{aligned} &D_E : \Omega \times \mathrm{T} \to \mathrm{IR} \\ &\left(\mathrm{t}, \omega\right) \mapsto D_E(\mathrm{t}, \omega) = \sqrt{\left(U(t,\omega) - \overline{U}(t)\right)\left(U(t,\omega) - \overline{U}(t)\right)^T} \end{aligned} \tag{6}$$

3.2 Mahalanobis distance

In statistics, the Mahalanobis distance is a measurement of distance introduced by P.C Mahalanobis in 1936. It is based on the correlation between variables by which various models can be identified and analyzed. This distance is associated with particular metric called Mahalanobis metric. It is a distance to the probabilistic direction between a measurement and a Gaussian probability law. Therefore, it is usable when one can approximate the distribution of the data by a normal law. One made tests of adequacy to show that the distribution of the observations data follow a normal law.

The characteristic of this distance is to estimate the deviation between a reference trajectory and an observed trajectory even if the components of the trajectory don't have the same magnitude. It grants a less important weight to the most disturbed components. It is also a method of dissimilarity measurement between two random vectors of same sample.
In practice, we suppose that one has *L* observations of the process U(t) in the discretizations $0 = t_0 < t_1 < \ldots < t_{M-1} = T$ of the interval *[0, T]*.

In these conditions, one can define the Mahalanobis distance between vector $\overline{U}$ of the reference observations and vector U of the discrete observations of the m[th] trajectory by:

$$D_M = d\left(U,\overline{U}\right) = \sqrt{\left[\left(U-\overline{U}\right)^T \Sigma^{-1} \left(U-\overline{U}\right)\right]} \tag{7}$$

Where Σ is a variance-covariance matrix of the random vector $\left(U,\overline{U}\right)$.
The projection of a vectorial process U(t) give a scalar process $D_M(t)$ defined by :

$$\begin{gathered} D_M : \Omega \times T \to IR \\ (t,\omega) \to D_M = \sqrt{\left[\left(U(t,\omega)-\overline{U}(t)\right)^T \Sigma^{-1} \left(U(t,\omega)-\overline{U}(t)\right)\right]} \end{gathered} \tag{8}$$

3.3 Application

To illustrate our remarks at the distances between trajectories, the figure (2) shows an example of distance calculation with the methods (Mahalanobis and Euclidean). These two distances represent the deviation between reference trajectory (or average) and the observed trajectories.

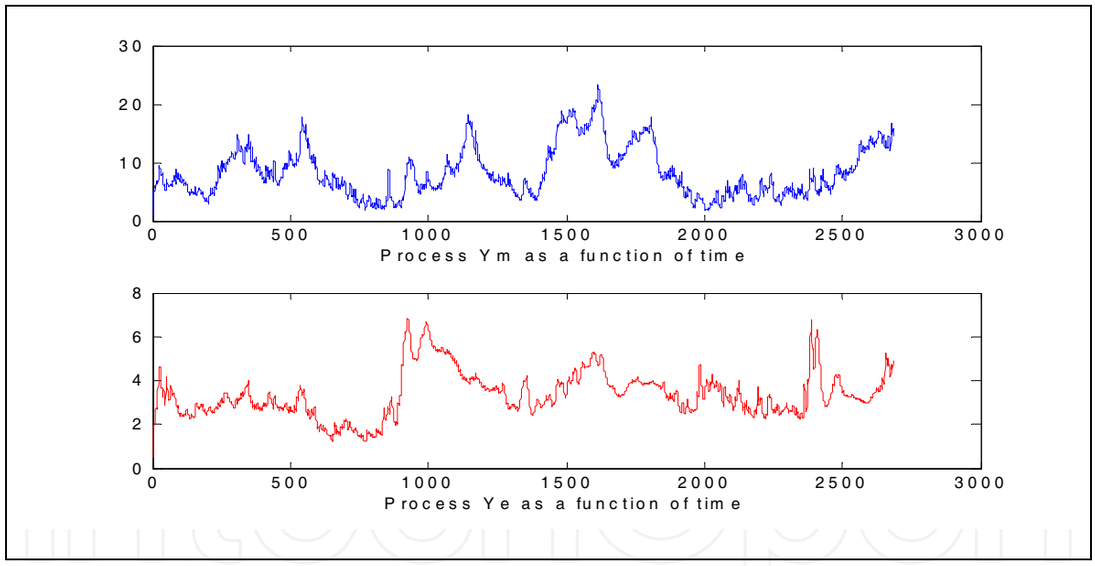

Fig. 2. Distance between trajectories

We can notice the existence of similarity zones between the scalar processes $D_M(t)$ and $D_E(t)$ in the figure (2) but also great differences exist sometimes. This first result explains that the correlation between the parameters can play a very important role. Therefore, a significant difference between both methods exists. We note that the Euclidean distance D_E is less sensitive to the parameters variations than the Mahalanobis distance D_M.

The figure (3) represents the temporal mean and standard deviation of the processes $D_E(\omega,t)$ and $D_M(\omega,t)$. In blue, we have the Mahalanobis distance and in red the Euclidean distance.

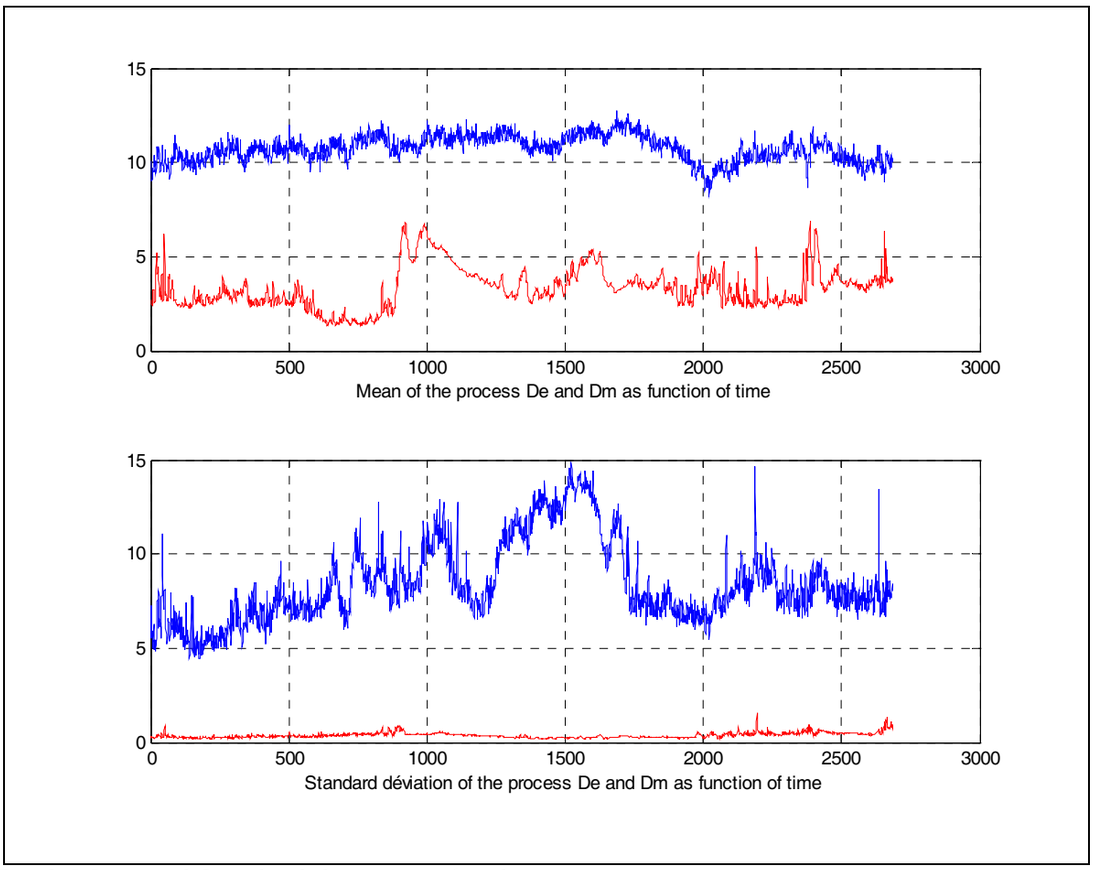

Fig. 3. Mean and Standard deviation of scalar processes

The figure (3) shows that these functions vary according to time and present a difference between them. We also notice that the processes are positive by construction because being distances thus they are not centered.

In order to obtain a centered scalar process, we have done a new transformation on the processes $D_M(t)$ and $D_E(t)$. We obtained the centered scalar processes $Y_m(t) = D_M(w,t) - m_{Dm}(t)$ and $Y_e(t) = D_E(w,t) - m_{De}(t)$. Where $m_{Dm}(t)$ and $m_{De}(t)$ are the average distance of the processes $D_M(w,t)$ and $D_E(w,t)$. The next step consists of doing a statistic analysis of these scalar processes.

4. Scalar process analysis

In this part, at first we will check the stationarity assumptions of scalar processes $Y_M(t)$ and $Y_E(t)$. Then, in the second section, we will describe the characterization of these processes. Afterwards, a third section will make it possible to identify the law of these processes. Lastly, a fourth section we will identify the law of maximum processes.

4.1 Stationary and ergodicity analysis

That is to say a function Y(t) with ($t \in R_+$) : Y(t) is a function or a random process, for each time t_1 fixed, $Y(t_1)$ is a random variable. The process Y(t) is entirely characterized (in probability) if one knows the probability density function (pdf) united multivariate of all finite collection (vector). (Bouleau, 1994)

$$Y_E=\{Y(t_1), Y(t_2),\ldots. Y(t_i),\ldots. Y(t_M)\} \text{ and } Y_M=\{Y(t_1), Y(t_2),\ldots. Y(t_i),\ldots. Y(t_M)\} \quad (9)$$

For all t_i and finite M.

After having defined a stochastic process, it is necessary to check the assumptions of stationarity and ergodicity of the scalar process Y(t). A random process is stationary by definition, if its moments are invariants by translation of time. We checked this assumption of two-order stationarity on our observations data by calculating the mean, the variance and the auto covariance function of the process Y(t). (Kree, 1983). By construction, the average and the variance are respectively equal to zero and the unit because the process was standardizes.

$$m_Y \equiv IE(Y(\omega,t)) = 0 = \text{constante } (\forall t) \text{ and } Var(Y(\omega,t)) = \sigma^2_Y = 1 = \text{constante } (\forall t) \quad (10)$$

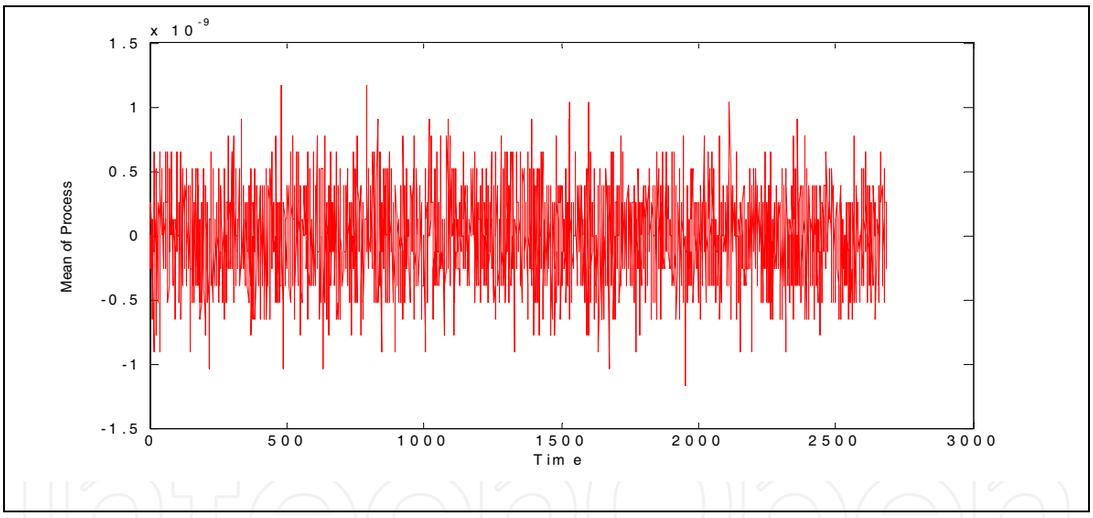

Fig. 4. Mean of the centered scalar process as a function of time (ms).

The auto-covariance function $C_Y(t_1,t_2)$, is the function of two variables t1 and t2 given by :

$$\begin{aligned} &C_Y : R\times R \to R \\ &(t_1,t_2) \to C_Y(t_1,t_2) = Cov(Y(t),Y(t+\delta)) = C_{YY}(t_{i+1}-t_i) = C_{YY}(\delta) \\ &\delta = t_{i+1}-t_i \end{aligned} \quad (11)$$

The figure (5) represents the auto-covariance function of processes D_E et D_M

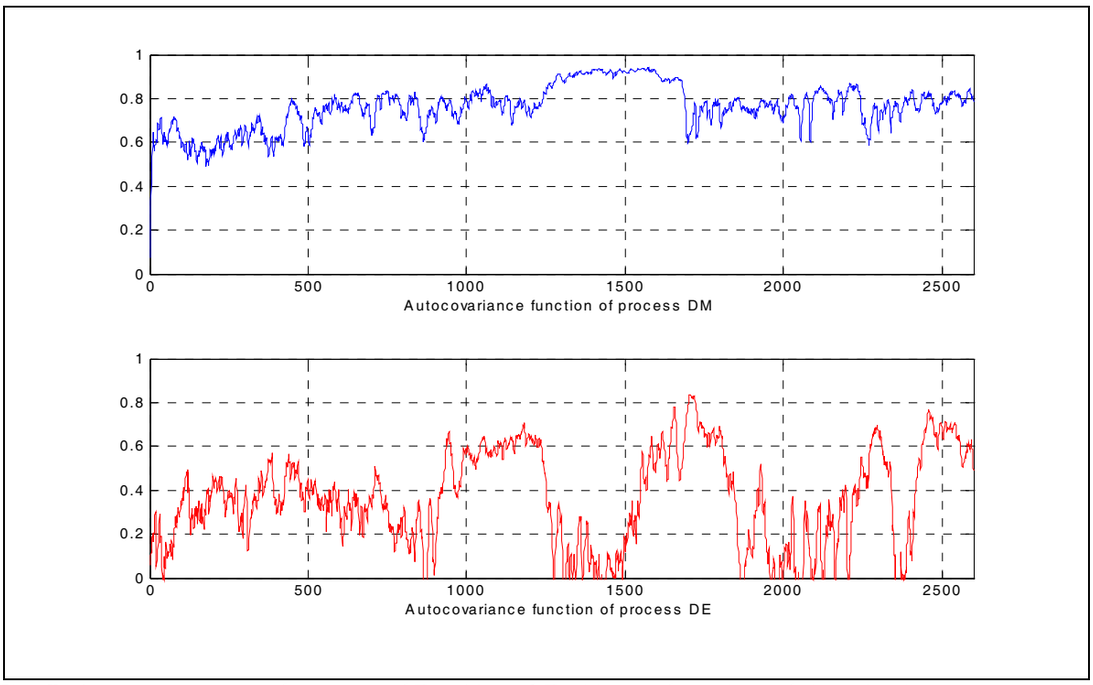

Fig. 5. Auto-covariance function of Dm(t) and De(t) as a function of time (ms).

We have just shown that the average, the standard deviation and the auto-covariance function do not depend on time. Thus, the processes $Y_M(t)$ and $Y_E(t)$ are stationary with order 2. After having checked the assumption of stationarity of the process, it is interesting to check the assumption of the process ergodicity. A process is ergodic, if the equivalence between the overall average (mean) and the space average on an infinite interval is verified:

$$m_Y \equiv E\left(Y(\omega,t)\right) \Leftrightarrow m_Y = \lim_{T \to \infty} \frac{1}{T} \int_0^T Y(s)ds = \text{constante} \quad (12)$$

By checking the assumption on our observations data, we note that it is checked. After having checked these assumptions, we use also a statistical test of stationarity (Xiao, 2007),

4.2 Scalar process characterization

To characterize processes Y_M and Y_E, we will estimate the power spectral density, the probability density and the function of distribution (Soize, 2000).

Power Spectral Density function Estimate

The objective of this section consists in considering the Power Spectral Density of the process Y(t) in order to be able to generate trajectories resulting from the same process. In referent in the preceding section of this study, it was checked that the process Y(t) is stationary at second-order. A transformation was made on the scalar process of kind have a new centered process. The PSD is obtained by using this following formula:

$$\hat{S}_{L,T}(\omega) = \frac{1}{2\pi}\frac{1}{L}\sum_{l=1}^{L}\left|\hat{X}^{l}(\omega)\right|^{2}$$
$$\hat{X}^{l}(\omega) = \int_{0}^{T} W_{T}(t)X^{l}(t)e^{-i\omega t}\,dt \qquad (13)$$

Where W_T is a temporal window (Hamming model). For l=1….L , where L is the number of trajectories in the class. The figure (6) shows estimated Power Spectral Density of Y_m and Y_e. We have obtained negative PSD because we have used log function to make a zoom on the figures.

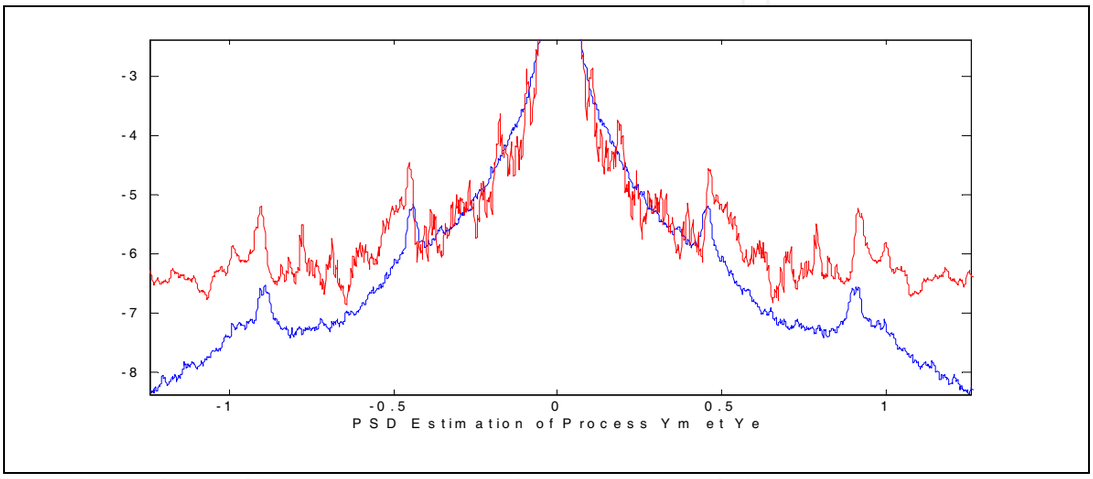

Fig. 6. Power Spectral Density estimates of the process Y_e and Y_m.

The red and blue curves correspond respectively to the PSD of the processes Y_m and Y_e.

Probability Density function Estimate

As previously, to characterize the processes $Y_m(t)$ and $Y_e(t)$ in a complete way, it is necessary to estimate its probability density P_Y and its distribution function F_Y. Estimated P_Y and F_Y are then defined by the following relations:

$$\left\{\begin{array}{l}\hat{P}_{X}^{M}(x) = \sum_{j\in J_M}\frac{N_j}{\delta N}1\mathrm{I}_{D_J}(x);\ \mathrm{x}\in\overline{\mathrm{X}}\\ \hat{F}_{X}^{M}(x) = \sum_{j\in J_M}\frac{\sum_{k=1}^{j}N_j}{N}1\mathrm{I}_{D_J}(x);\ \mathrm{x}\in\overline{\mathrm{X}}\end{array}\right\} \qquad (14)$$

Where $1I_{Dj}$ is a indicator function of D_j

The two curves in the figure (7) represent the probability density function of the processes $Y_m(t)$ and Ye(t). The probability density of the process $Y_m(t)$ tends towards a Gamma law whereas the process $Y_e(t)$ tends towards a Gaussian law.

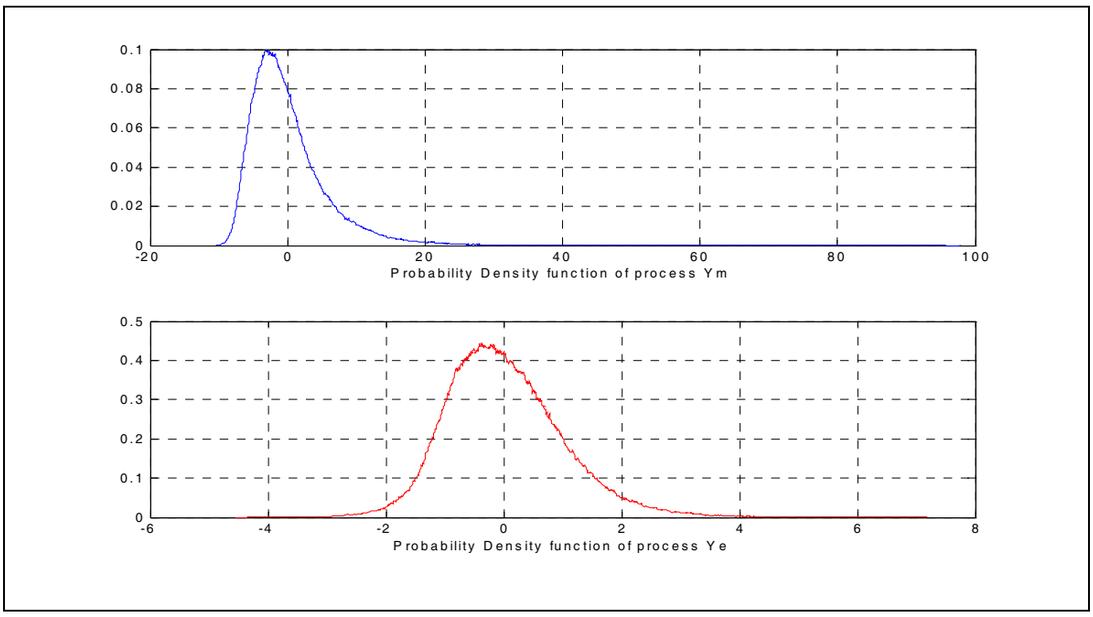

Fig. 7. Probability Density function of Y_m and Y_e.

Distribution function Estimate

The two curves in the figure (8) represent the distribution function of the processes Y_m and Y_e. We note a big difference between them as in the probability density.

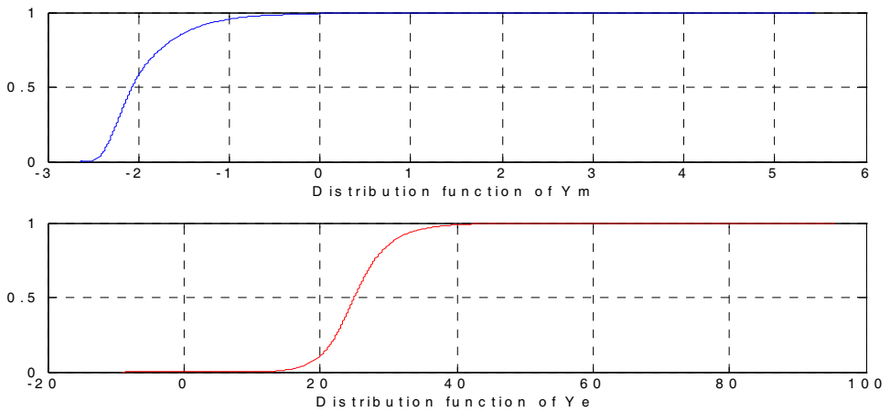

Fig. 8. Distribution function of processes Y_m and Y_e.

After the characterization of process $Y_E(t)$ and $Y_M(t)$, the next section will consist to identify the scalar process $Y_E(t)$ and $Y_M(t)$.

4.3 Scalar process identification

We initially calculated the kurtosis (K) and skewness (S) coefficients to have an idea of the classical probability laws to use for the approximation of the processes $Y_E(t)$ and $Y_M(t)$ laws.

Kurtosis coefficient

The kurtosis coefficient is a statistic which measures the degree of probability of the extreme events. More, it is large, more the tails of distribution are thick compared to those of the normal law, i.e. more of the extreme events can potentially occur. This coefficient noted K is calculated by:

$$K = \frac{\mu_X^4}{\sigma_X^4} - 3 \quad \text{where} \quad \mu_X^4 = \frac{\sum X_E^4}{N} \tag{15}$$

Skewness coefficient

The skewness coefficient measures the degree of asymmetry of the distribution. For a perfectly symmetrical distribution (for example, a normal law), the coefficient of asymmetry S= 0. If the coefficient S>0, the distribution is asymmetrical on the left: there is a strong probability that an event is with the top of the average that in lower part (the modal value is with the top of the average). If, the distribution is asymmetrical on the right: there is a weaker probability than an event is with the top of the average than in lower part (the modal value is with the lower part of the average). This coefficient noted S is calculated by the following equations:

$$K = \frac{\mu_X^3}{\sigma_X^3} \quad \text{where} \quad \mu_X^4 = \frac{\sum X_E^4}{N} \tag{16}$$

	Kurtosis	Skewness
Process Y_M	8.6970	2.5454
Process Y_E	3.84	1.5286

Table 1. Kurtosis and skewness coefficient of processes Y_E and Y_M

While referring on the one hand, visually on the figure (7) and on the other hand, by looking at the kurtosis and the skewness coefficients, we note that the laws of our processes can be approximated by classical laws (Bouleau, 1986). The use of the comparison criterions (Lelu, 2002) made it possible to choose the best approximations for the two laws characterized previously. The normal law was selected for the Euclidean distance and the Gumbel law for the Mahalanobis distance. The figure (9) represents the target law of probability of scalar processes $Y_M(t)$ and $Y_E(t)$ as well as the law of probability of the approximations of these processes.

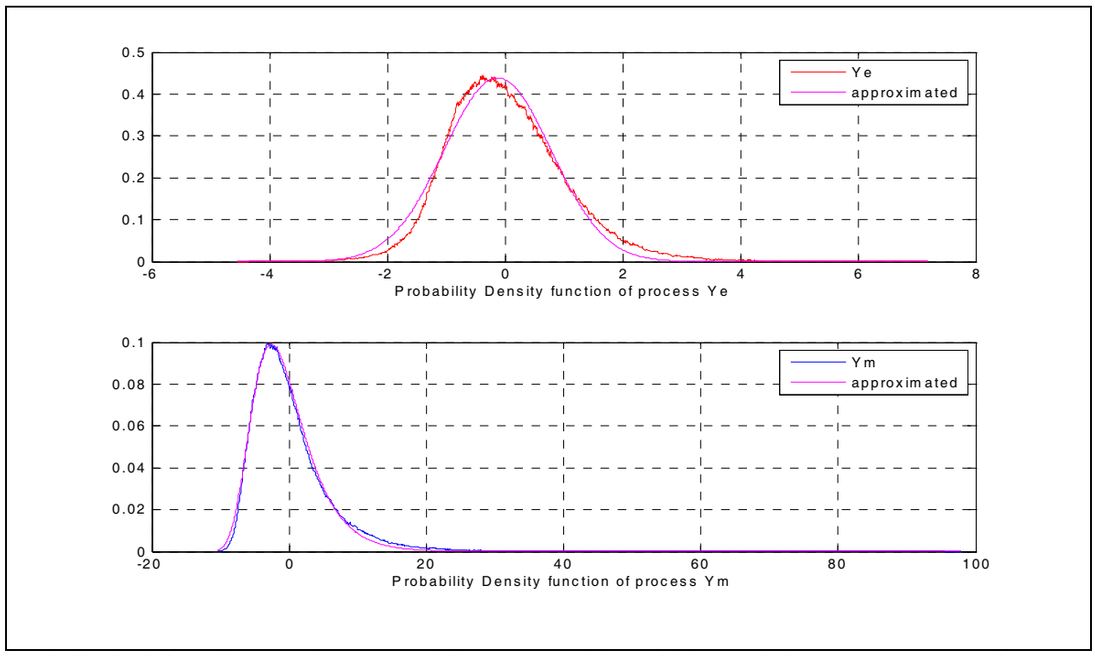

Fig. 9. Probability density function of the process Ye and Ym and their approximated

The figure (9) shows a better approximation for our laws especially for the Gumbel law. The theoretical laws obtained enable us to simulate distances between trajectories for the studied bend. These simulated distances will have the same statistical properties as the sample of distances which was used to build the model of distances. The figure (10) represents an example of distance obtained with the measured trajectories and another obtained by simulation of process $Y_E(t)$. The red curve corresponds to that obtained by the data of measurements and the blue one corresponds to that simulated.

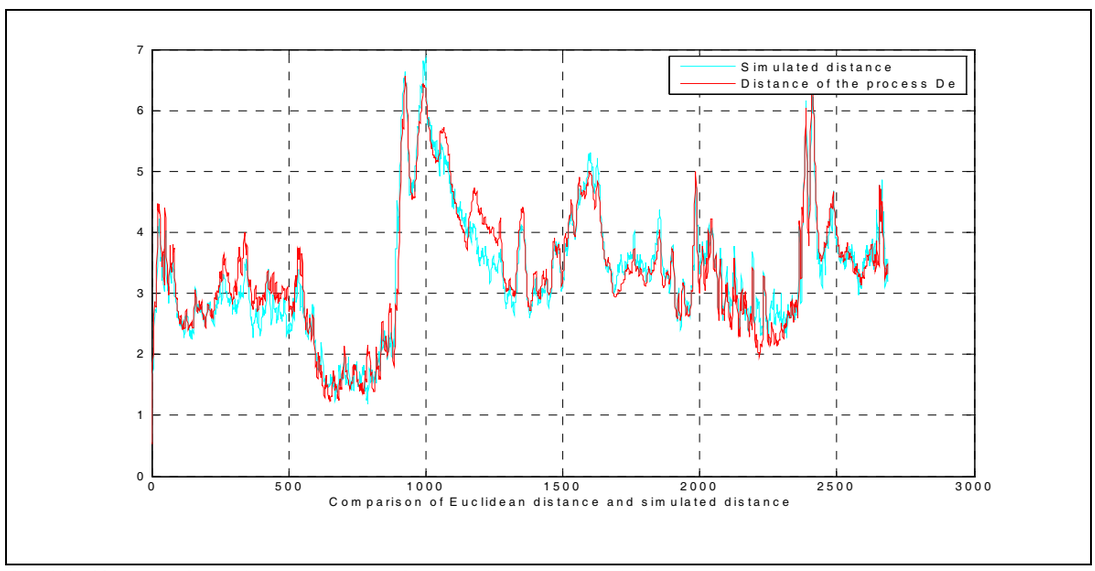

Fig. 10. Comparison between Euclidean distance and simulated distance

We can conclude that the model based on distances implemented is validated. The next section will be to identify the law of the maximum of processes $Y_E(t)$ and $Y_M(t)$.

4.4 Identification of process maximum law

In the section (1) of this part, we showed that scalar processes $Y_M(t,w)$ and $Y_E(t,w)$ respectively follow the law of Gumbel and the normal law. To estimate trajectory probability of failure, we will identify the law of maximum of the scalar processes $Y_E(t)$ and $Y_M(t)$. The purpose of the maximum law identification is to eliminate any temporal aspect along the bend.

According to the stability principle, if the law of an initial process is of type I, II or III, corresponding to a law of maximum, then the law of maximum is of the same type. The extreme law of type I (Gumbel) has as an asymptotic law of the maximum(Jacob, 1993). This law is represented by the following formula:

$$\begin{cases} F_n(x) = \exp\left[-e^{-(\alpha_n(x-u_n))}\right] \\ f_n(x) = \alpha_n e^{-(\alpha_n(x-u_n))} \exp\left[-e^{-(\alpha_n(x-u_n))}\right] \end{cases} \tag{17}$$

Where u_n is a location parameter, representing the mode (or the most probable value) of U_n and the characteristic value of X. $u_n\alpha_n$ measures the dispersion of this variable while α_n is the maximum intensity of X. The figure (11) represents the estimate of the law of the maximum of process Ye (T) and its approximation.

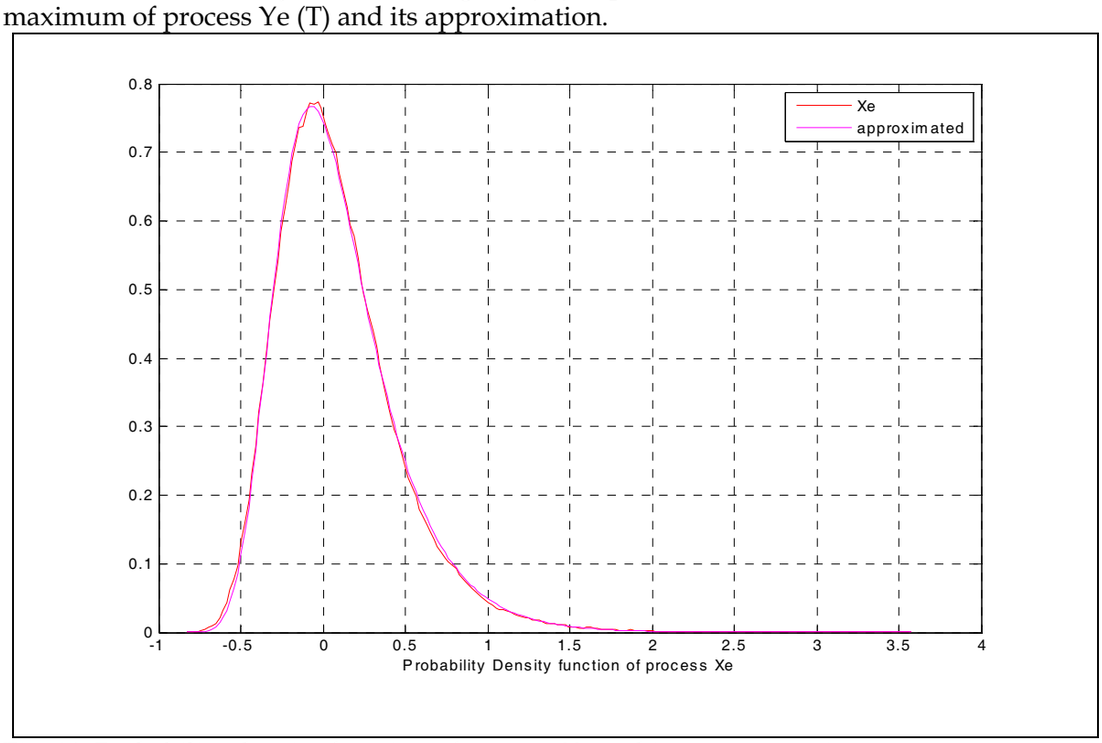

Fig. 11. Probability density function of process Xe and its approximation

We can conclude that the law of maximum of a Gaussian process is a law of Gumbel. For these laws of maximum, to estimate the trajectory probability of failure, it is necessary to define the trajectories limit states. The next step will be to determine these limit states.

5. Trajectory stability criteria

The final aim of this study is to estimate the trajectory probability of failure knowing its variation compared to the reference trajectory. For that, it is necessary to define the safety field of the trajectory. In this part, we will determine the trajectory criteria of stability. Then we will speak about the limit states of the trajectories. Finally we will calculate the threshold distance $D_{threshold}$ not to be exceeded to remain in safety.

5.1 Trajectories stability criterion

Security criteria

Safety criteria in longitudinal control can be treated as a problem to assure a minimal distance between vehicles. In this study, we will insist on the criterion of comfort.

Comfort criteria

Passenger comfort in public ground transportation is determined by the changes in motion felt in all directions, as well as by the other environmental effects. Typically, acceleration magnitude is taken as a comfort metric. Consequently, the jerk, i.e. the acceleration's derivate better reflects a human comfort criterion. As its name suggests, jerk is important when evaluating the destructive effect of a motion on a mechanism or the discomfort caused to passengers. The movement of delicate instruments needs to be kept within specified limits of jerk as well as acceleration to avoid damage.

In (Zakowska,2008) comfort due to motion changes in a vehicle's longitudinal direction has been treated; When designing a train and elevators, engineers will typically be required to keep the jerk less than (2 m/s^3) for passengers comfort. However, the bounded longitudinal jerk in this study is less than (3 m/s^3).

The main theoretical assumption is: a subject driving on a self-explaining road assumes a correct and safe trajectory and the local lateral accelerations depend only on the road curvature geometry. If the driver corrects the vehicle's trajectory more than what road curvature imposes, the road is not self-explaining and, consequently, it can be unsafe. If the local transversal accelerations do not depend only on the actual road curvature, they are biased by driver's corrections of trajectory. The local variability of lateral acceleration shows clearly the corrections of trajectory that the driver assumes and this could be so labeled as a discomfort index. These repeated local oscillations represent a violation of the driver expectancy. Authors have used formula (18) to estimate pathologic discomfort:

$$PD = \int_{s=0}^{s=L} \left| a_t(s) \right| ds \approx \sum_{j=0}^{N} \left| \left(\frac{\partial^2 y}{\partial t^2} \right)_j - \frac{\partial x / \partial t}{\rho_j} \right| \tag{18}$$

By applying this criterion to the representative sample of trajectories observed on the same studied turn, we obtained after standardization, PD ranging between (0.15 and 1). However, the bounded pathologic discomfort in this study is less than (0.75). All the trajectories which do not respect these two criteria are regarded as unstable.

5.2 Trajectories limit state

Constraints obtained through the preceding criteria give practical limits of variations for the vehicle kinematics parameters in security and comfort conditions. This subset D_S is made up of the trajectories which respect the comfort criterion.

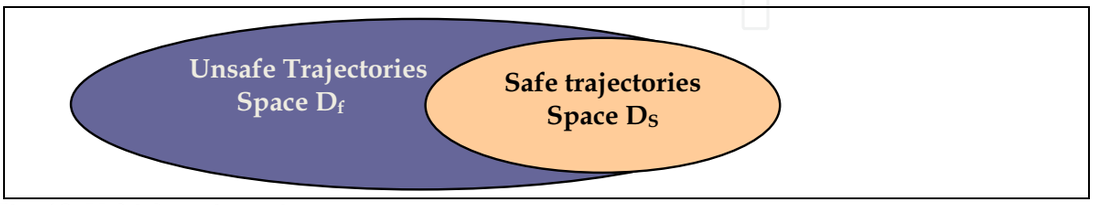

Fig. 12. Vehicle trajectories space

However, the bounded trajectory parameters are less than: {transversal position (2m), longitudinal speed (22m/s), lateral speed (9m/s), longitudinal acceleration (3m/s²) and lateral acceleration (4 m/s²)}.

5.3 Threshold Distance

The distances calculated starting from the observed trajectories lie between (0, 15). In this study, we choose a threshold distance equal to (10) beyond which the trajectory is unstable. This assumption is checked through the limit states previously definite. The figure (13) represents the delimitation zone of the safe distances and that of the unsafe distances. The two zones are separated by the distance threshold. This distance threshold will be used in the next step to estimate the trajectory probability of failure.

The last step of this study will consist to apply the analysis reliability of civil engineer.

6. Reliability analysis of trajectories

In this part of the chapter, we propose tools of the probabilistic reliability theory to assess safety indices of trajectories. The method consists to treat firstly the function of limit state and the transformation of the physical space variables towards the space of the normalized variables. Then, the reliability indice will be calculated. Lastly, as any analysis reliability engineer, one will evaluate the probability of failure (PF) associated with the selected limit state. We recall that the stationnarity assumption takes all its sense in this part to predict a failing trajectory.
We point out that the maximum of the process $Y_E(t)$ or $Y_M(t)$ is represented by:

$$Y(\omega) = \text{Sup}_{t\in[0,T]} \left| d(U(t,\omega), \overline{U}(t)) \right| \tag{19}$$

Y(ω) is a regular random variable for which one has a good approximation of his law. Let G : IR → IR ; x → G(x) = y – d where d is an element of IR+ and G is the limit state function.

We choose to define the safety and the failure events by :

$E_s = \{\omega \in \Omega \text{ such } G(X(\omega)) < 0\}$ and $E_f = \{\omega \in \Omega \text{ such } G(X(\omega)) \geq 0\}$

And the safety domain and the unsafe domain by :

$D_s = \{x \in IR \text{ such } G(x) < 0\}$ and $D_f = \{x \in IR \text{ such } G(x) \geq 0\}$

It acts, once known the probability density P_Y of the random variable X and after having defined the events E_s and E_f, it is necessary to calculate the probabilities $P(E_s)$ and $P(E_f)$. We obtain :

$$P_f = P(E_f) = \int_{D_f} p_Y(y)dy \quad \text{and} \quad P(E_s) = 1\text{-}P(E_f) \tag{20}$$

This is why, one interests only in the estimate of P_f

We based then on a classical result of the probabilities calculation which says that under certain conditions (that we will suppose satisfied here), one can always build a regular transformation T such as if X is a Gaussian v.a. standard with values in IR, then one with the equality in law Z= T (X). The safety and the failure events are written by:

$E_s = \{\omega \in \Omega \text{ such } \Gamma(Z(\omega)) < 0\}$ and $E_f = \{\omega \in \Omega \text{ such } \Gamma(Z(\omega)) \geq 0\}$, where $\Gamma = GoT^{-1}$

The images per T of the safety and failure fields are written as for them:

$\Delta_S = T(D_s) = \{x \in IR \text{ such } \Gamma(x)) < 0\}$ and $\Delta_f = T(D_f) = \{y \in IR \text{ such } \Gamma(y)) < 0\}$

One has then:

$$P_f = \int_{IR} 1_{\Delta_f}(x) p_X(x)dx \quad \text{where} \quad p_X(x) = \frac{e^{-x^2/2}}{\sqrt{2\pi}} \tag{21}$$

The law of Y being known it is possible to obtain an approximation of PF either by using a method of the Monte Carlo type or by using methods of approximation (FORM and SORM methods) (Lemaire, 2005). For that we must initially define the index of Hasofer-Lind:

$\beta_{HL} = d(O, \Delta_f)$ where O is origin point of IR. To get β_{HL} consists to solve the following problem:

$$\begin{cases} \text{Find } y^* \in IR \text{ such that :} \\ \|y^*\| = \underset{y \in \Delta_f}{Min} \|y\| \end{cases} \tag{22}$$

FORM method

Elle consiste à effectuer une approximation du 1er ordre de Δ_f au voisinage de y*

$$P_f \text{ est approchée par } P_f^L = \Phi(-\beta_{HL}) \quad \text{avec} \quad \beta_{HL} = \frac{\Gamma(y^*) - \langle \nabla\Gamma(y^*), y^* \rangle}{\|\nabla\Gamma(y^*)\|}$$

and Φ is the distribution function of Gaussian law in IR.

SORM Method

It consists in carrying out a second order approximation of Δ_f in au voisinage de y*

We can use for example the following approximation (due à Breitung):

$$P_f^L \approx \Phi(-\beta_{HL}) \left| \sum_{i=1}^{d-1} (1 - \beta_{HL} \chi_i(y^*) \right|^{-1/2}$$

avec $\chi_i(y^*),\ i = 1,...,d-1$ les courbures principales de Γ_Q au design point y^*

7. Conclusion

The goal of this chapter was to estimate the trajectory probability of failure by using metric (or distance) between the trajectories starting from data of experimental measurements.

Initially, after having defined the trajectory of the vehicle and its properties, we considered a sample of trajectories resulting from the same stochastic process vectorial. The trajectories of the process are the solutions of a stochastic differential equation controlled by the system of control. Then, we projected the dated measurements of this process on IR in order to bring back to have scalar problem. This step passes by the use of judiciously selected functional (one based on the use of the Euclidean distance, the other based on the use of the Mahalanobis distance).

Afterwards, we considered the process (scalar) of deviations with the average distance of the sample. It is this process which we sought to characterize. An statistical analysis was carried out on this scalar process with an aim of studying the stationnarity. The stationnarity assumption was not rejected for these processes.

Then, to identify the model of distance between trajectories, on the one hand, we characterized each process by estimating the probability law, the function of distribution and the power spectral density. In addition, we identified the laws of probability of each process by a reasonable approximation. The validation of this approximation was made by using the integral criterion.

Then, after having identified the law of maximum of the two preceding laws and by using of the safety and comfort criteria of the trajectory, we estimated the probability of failure.

Finally, we present simulation results of the proposed methods. The validation is carried out by means of experimental measures.

8. References

Bouleau, N., 2002, «*Probabilités de l'ingénieur. Variables aléatoires et simulation*», Hermann, 383 pages. ISBN : 2-7056-6430-4

Bouleau, N., 1988, «*Processus stochastiques et applications*», Hermann, ISBN : 2-7056-1420-20

Jacob, B., 1993, «*Approximation de la loi des valeurs extrêmes*», Cours de genie civil, Ecole Nationale des Ponts et Chaussées, France

Arai, T. & Kragic, D. (1999). Name of paper, In: *Name of Book in Italics,* Name(s) of Editor(s), (Ed.), page numbers (first-last), Publisher, ISBN, Place of publication

Lauffenburger, J. Ph.; Basset, M.; Coch, F. and Gissinger, G. L., «*Driver-aid system using Path planning for lateral vehicle control*», 2003, Control Engineering Practice, volume 11/2, Février, pp. 215-229.

Koita, A. and Daucher, D., 2008, «*Protocole expérimental : recueil de données de mesures de trajectoires en virage*» , rapport interne LCPC.

Koita, A. and Daucher, D., 2009, «*Stochastic Analysis of Vehicle Trajectories in Bend: toward a risk indicator construction*», ICOSSAR 2009, International Conference on Structural Safety and Reliability, September 13-17, Osaka, Japan.

Kanayama, Y. and Hartman, B., 1997, «*Smooth local path planning for autonomous vehicles*», Int. Robotics Research, Vol. 16 No. 3, pp. 263.84

Kree, P. and Soize, C. 1983. «*Mathematics of random phenomena*», Dordrecht

Lelu, A., 2002, «*Comparaison de trois mesures de similarité utilisées en documentation automatique et analyse textuelle*» JADT., coord. IRISA, St. Malo, 13-15 Mars 2002

Lanequel, L. 1992. *Euclidean distance matrix analysis of the muzzle region in Adapis*. ISSN 0764 - 4450, vol 314. N 12, pp 1387-1393.

Lauffenberger, J. P. 2002. *Contribution à la surveillance temps réel du système, conducteur - vehicule-environnement, élaboration d'un système d'aide à la conduite*. Université Haute Alsace, Mulhouse. PHD Thesis

Lemaire, M., 2005, «*Fiabilité des structures, Couplage Mécano-.abiliste statique*», Hermes, 2005, ISBN 2-7462-1057-6

Pugachev, V., 1982, «*Théorie des probabilités et statistique mathématique*», Moscou, Edition MIR,

Soize, C., 1993, «*Méthodes mathématiques en analyse du signal*», MASSON, 1993

Takahashi, A.; Hongo, T. and Ninomiya, Y. «*Local Path Planning and Motion Control for AGV in Positionning*», Proc. IROS, pp 392-395, Tsukuba, Japan

World Mortality Database. «*WHO Mortality statistics. World Health Organization*», 2004.

Xiao J., P. Borgnat, P. Flandrin, 2007: "*Testing stationarity with time-frequency surrogates*," XVth European Signal Proc. Conf. EUSIPCO-07, Poznan

Xinrong Z. Huili, Z and Yongxin, Y. 2001. «*Mahalanobis distance image segmentation based on two-dimensional histogram*. SPIE Journal proceedings, ISBN 0-8194-4278-X

Zakowska, L.; Benedetto, A.; Calvi, A and D'Amico, F., 2009, «*The Effect of curve Characteristics on driving behavior: a driving simulator study*», TRB 88 th Annual Meeting (January 11-15, 2009) USA

IntechOpen

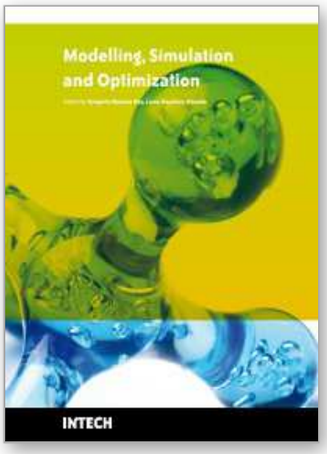

Modelling Simulation and Optimization

Edited by Gregorio Romero Rey and Luisa Martinez Muneta

ISBN 978-953-307-048-3
Hard cover, 708 pages
Publisher InTech
Published online 01, February, 2010
Published in print edition February, 2010

Computer-Aided Design and system analysis aim to find mathematical models that allow emulating the behaviour of components and facilities. The high competitiveness in industry, the little time available for product development and the high cost in terms of time and money of producing the initial prototypes means that the computer-aided design and analysis of products are taking on major importance. On the other hand, in most areas of engineering the components of a system are interconnected and belong to different domains of physics (mechanics, electrics, hydraulics, thermal...). When developing a complete multidisciplinary system, it needs to integrate a design procedure to ensure that it will be successfully achieved. Engineering systems require an analysis of their dynamic behaviour (evolution over time or path of their different variables). The purpose of modelling and simulating dynamic systems is to generate a set of algebraic and differential equations or a mathematical model. In order to perform rapid product optimisation iterations, the models must be formulated and evaluated in the most efficient way. Automated environments contribute to this. One of the pioneers of simulation technology in medicine defines simulation as a technique, not a technology, that replaces real experiences with guided experiences reproducing important aspects of the real world in a fully interactive fashion [iii]. In the following chapters the reader will be introduced to the world of simulation in topics of current interest such as medicine, military purposes and their use in industry for diverse applications that range from the use of networks to combining thermal, chemical or electrical aspects, among others. We hope that after reading the different sections of this book we will have succeeded in bringing across what the scientific community is doing in the field of simulation and that it will be to your interest and liking. Lastly, we would like to thank all the authors for their excellent contributions in the different areas of simulation.

INTECH
open science | open minds

InTech Europe
University Campus STeP Ri
Slavka Krautzeka 83/A

InTech China
Unit 405, Office Block, Hotel Equatorial Shanghai
No.65, Yan An Road (West), Shanghai, 200040, China

www.intechopen.com

51000 Rijeka, Croatia
Phone: +385 (51) 770 447
Fax: +385 (51) 686 166
www.intechopen.com

中国上海市延安西路65号上海国际贵都大饭店办公楼405单元
Phone: +86-21-62489820
Fax: +86-21-62489821

IntechOpen

IntechOpen